Acknowledgements

Contents

Chapter 1

Introduction

The relationship between physics and finance is a long-standing one. [Bachelier, 1900] is perhaps the first example of a model developed by physicists (Brownian motion) being applied to financial markets, specifically to the pricing of derivative products. This work would remain largely unnoticed until [Black and Scholes, 1973] was published, now considered the foundation of modern quantitative finance.

Beyond derivative pricing, econophysics has been active since the 1990s, applying methods from statistical physics to a wide range of problems in economics and finance. For example, [Bouchaud and Mézard, 2000] examines the distribution of wealth in a simplified economy, mapping it to the random 'directed polymer' problem.

Econophysics emerged as a distinct interdisciplinary field when physicists began to systematically apply concepts from statistical mechanics, complex systems, and nonlinear dynamics to economic and financial systems. The motivation comes from the observation that financial markets, like physical systems, are composed of many interacting agents whose collective behavior gives rise to emergent phenomena such as bubbles, crashes, and fat-tailed return distributions.

For an introduction to econophysics, see [Mantegna and Stanley, 1999] and [Sharma et al., 2011].

The scope of this thesis is to explore how concepts and models from statistical physics, particularly spin models, can be used to gain insight into the collective behavior observed in financial markets. After introducing the necessary background in financial mathematics and statistical mechanics, we focus on the Bornholdt model, a spin-based agent model that captures both trend-following and contrarian strategies. Through analytical discussion and numerical simulations, we investigate how this model reproduces key stylized facts of financial time series, such as volatility clustering and fat-tailed return distributions, highlighting the strengths and limitations of physics-inspired approaches to financial market dynamics.

Chapter 2

Background and theoretical framework

2.1 Financial mathematics: option pricing

In this section, we will first provide a brief introduction to the language of financial mathematics in continuous time, and then introduce the Black-Scholes model for option pricing.

2.1.1 Setting

Let us assume we have a financial market on which a bond B and a stock S are traded. We will describe the dynamics of the price of each asset in a continuous time setting. We will assume that the bond B has a deterministic return r:

$$dB(t) = rB(t)dt \tag{2.1}$$

On the other hand, we will assume that the stock S follows a geometric Brownian motion:

$$dS(t) = \mu S(t)dt + \sigma S(t)dW(t) \tag{2.2}$$

Where $W(t)$ is a standard Brownian motion, μ is the drift, and σ is the volatility. The drift μ is the expected return of the stock, and the volatility σ is a measure of the uncertainty of the stock price.

On this setting, we can go ahead and define what a european call option is:

Definition 1. *A european call option is a contract that gives the holder the right, but not the obligation, to buy an asset at a specified price (the strike price) at a specified time (the*

expiration date). The payoff of a european call option at time t is given by:

$$X(t) = \begin{cases} max(S(t) - K, 0) & \text{if } t = T \\ 0 & \text{if } t < T \end{cases} \tag{2.3}$$

Where $S(t)$ is the price of the underlying asset at time t, K is the strike price, and T is the expiration date. The payoff is zero if the option is not exercised, and it is equal to the difference between the price of the underlying asset and the strike price if the option is exercised.

The question we want to answer is: what is the fair price of a european call option? Let us define $C(t)$ as the price of a european call option with expiration T and strike price K. We will then work on the market $\mathcal{M} = \{B(t), S(t), C(t)\}_{t \in \mathcal{T}}$, where $\mathcal{T}$ is the set of trading times and $B(t)$ and $S(t)$ as defined above. Formally, the question we are asking is what is the fair value of $C(t)$? In order to answer this question, we will introduce no-arbitrage pricing.

2.1.2 No arbitrage pricing

On the market $\mathcal{M} = \{B(t), S(t), C(t)\}_{t \in \mathcal{T}}$, we define a portfolio $h(t) = [h_B(t), h_S(t), h_C(t)]$, where each $h_i(t), i \in \{B, S, C\}$ is the number of units of asset i held at time t.

Definition 2. *Given a portfolio $h(t)$, its value process $V(t)$ is given by:*

$$V^h(t) = h_B(t)B(t) + h_S(t)S(t) + h_C(t)C(t), \quad \forall t \in \mathcal{T} \tag{2.4}$$

The value process is then the total value of the portfolio at each time t.

Definition 3. *A portfolio is said to be self-financing if the value process of the portfolio satisfies the following equation:*

$$dV^h(t) = h_B(t)dB(t) + h_S(t)dS(t) + h_C(t)dC(t) \tag{2.5}$$

This means that the change in the value of the portfolio is equal to the sum of the changes in the value of each asset, weighted by the number of units held in each asset. Intuitively, a self-financing portfolio is one in which the changes in the value of the portfolio are due to the changes in the value of the assets, and not due to any additional investments or withdrawals.

Definition 4. *An arbitrage opportunity is a self-financing portfolio $h(t)$ such that the following conditions hold:*

1. $V^h(0) = 0$.

2. $P(V^h(T) \geq 0) = 1$.

3. $P(V^h(T) > 0) > 0$.

Meaning that the portfolio has zero initial value, it is non-negative at time T, and it has a positive probability of being strictly positive at time T. Intuitively, an arbitrage opportunity is a way to make a sure profit without any initial investment.

We will assume that the market $\mathcal{M}(t)$ is arbitrage free, meaning that there are no arbitrage opportunities on the market at any $t \in \mathcal{T}$. We introduce one last lemma before moving to the pricing of european call options.

Lemma 1. *Suppose that in an arbitrage-free market there exists a self-financing portfolio $h(t)$ such that $dV^h(t) = kV^h(t)dt$, where k is a constant. Then, the return k is equal to the risk-free rate r.*

Proof. Assume WLOG $B(0) = 1$. Assume $V^h(0) > 0$ and $k > r$. Other cases are either equivalent or equivalent by reversing the portfolio position. Let us construct a portfolio $h'(t)$ consisting of one unit of the self-financing portfolio $h(t)$ and $-V^h(0)$ units of the risk-free asset $B(t)$, such that:

$$V^{h'}(0) = V^h(0) - V^h(0) = 0 \tag{2.6}$$

At $t > 0$:

$$\begin{aligned} V^{h'}(t) &= V^h(t) - V^h(0)B(t) \\ &= V^h(0)e^{kt} - V^h(0)e^{rt} \\ &= V^h(0)(e^{kt} - e^{rt}) > 0 \end{aligned} \tag{2.7}$$

Which makes $h'(t)$ an arbitrage opportunity, which is a contradiction. Therefore, we must have $k = r$. □

2.1.3 The Black-Scholes model

Assumptions

The Black-Scholes model is a mathematical model for the pricing of european options, introduced in [Black and Scholes, 1973]. The assumptions for deriving the price of the option are:

Assumption 1. *There exists a locally riskless asset with known and constant return, as we introduced it in Equation 2.1:*

$$dB(t) = rB(t)dt$$

Where r is the risk-free return.

Assumption 2. *The risky asset follows a geometric Brownian motion, as we untroduced it in Equation 2.2:*

$$dS(t) = \mu S(t)dt + \sigma S(t)dW(t)$$

Where $W(t)$ is a standard Brownian motion, μ is the constant drift, and σ is the volatility of the asset.

Assumption 3. *The market $\mathcal{M}(t)$ is arbitrage-free.*

Assumption 4. *The market is frictionless, meaning that there are no transaction costs, and the assets can be traded continuously.*

Assumption 5. *The stock $S(t)$ pays no dividends.*

Assumption 6. *It is possible to short-sell the asset without any restrictions or penalties.*

Assumption 7. *It is possible to borrow any fraction of the security at the risk-free rate.*

Derivation

Let $C(S,t)$ be the price of a European call option written on the underlying asset $S(t)$.

Applying Itô's Lemma to $C(S,t)$, we have:

$$dC = \frac{\partial C}{\partial t}dt + \frac{\partial C}{\partial S}dS + \frac{1}{2}\frac{\partial^2 C}{\partial S^2}dS^2$$

Substitute the dynamics of $S(t)$:

$$dS = \mu S dt + \sigma S dW$$

$$dS^2 = (\sigma S)^2 dt = \sigma^2 S^2 dt$$

Thus:

$$dC = \frac{\partial C}{\partial t}dt + \frac{\partial C}{\partial S}(\mu S dt + \sigma S dW) + \frac{1}{2}\frac{\partial^2 C}{\partial S^2}\sigma^2 S^2 dt$$

Simplify:

$$dC = \left(\frac{\partial C}{\partial t} + \mu S\frac{\partial C}{\partial S} + \frac{1}{2}\sigma^2 S^2\frac{\partial^2 C}{\partial S^2}\right)dt + \sigma S\frac{\partial C}{\partial S}dW$$

Now, construct a hedged portfolio $\Pi = C - \Delta S$, where $\Delta = \frac{\partial C}{\partial S}$. The change in the portfolio is:

$$d\Pi = dC - \Delta dS$$

Substituting:

$$d\Pi = \left(\frac{\partial C}{\partial t} + \frac{1}{2}\sigma^2 S^2\frac{\partial^2 C}{\partial S^2}\right)dt$$

Note that the dW terms cancel because:

$$\sigma S \frac{\partial C}{\partial S} dW - \frac{\partial C}{\partial S} \sigma S dW = 0$$

This portfolio is riskless, and by Lemma 1, it must grow at the risk-free rate:

$$d\Pi = r\Pi dt = r(C - \Delta S)dt$$

Equating both expressions for $d\Pi$:

$$\left(\frac{\partial C}{\partial t} + \frac{1}{2}\sigma^2 S^2 \frac{\partial^2 C}{\partial S^2} \right) dt = r \left(C - S \frac{\partial C}{\partial S} \right) dt$$

Cancelling dt and rearranging terms:

$$\frac{\partial C}{\partial t} + \frac{1}{2}\sigma^2 S^2 \frac{\partial^2 C}{\partial S^2} + rS \frac{\partial C}{\partial S} - rC = 0$$

This is the Black-Scholes partial differential equation.

Formula

The Black-Scholes formula for a European call option with strike price K, time to maturity $T - t$, and current underlying price S is:

$$C(S, t) = S\Phi(d_1) - Ke^{-r(T-t)}\Phi(d_2)$$

where:

$$d_1 = \frac{\ln(S/K) + (r + \frac{1}{2}\sigma^2)(T - t)}{\sigma\sqrt{T - t}}, \quad d_2 = \frac{\ln(S/K) + (r - \frac{1}{2}\sigma^2)(T - t)}{\sigma\sqrt{T - t}}$$

and $\Phi(\cdot)$ is the cumulative distribution function of the standard normal distribution.

2.1.4 Discussion

The Black-Scholes model relies on several key assumptions, one of which is Assumption 2: the price of the underlying asset follows a geometric Brownian motion with constant volatility. While this assumption is mathematically convenient and allows for an analytical solution to the pricing problem, it does not always align with empirical observations of financial markets.

In practice, the distribution of asset returns often exhibits fat tails, meaning that extreme events (large positive or negative returns) occur more frequently than predicted by a normal distribution. Furthermore, returns are not always independent over time; they

often exhibit autocorrelation, which violates the assumption of independent increments in the geometric Brownian motion.

These discrepancies have significant implications. For instance, the assumption of normally distributed returns can lead to an underestimation of the probability and impact of extreme market events, such as the 1987 stock market crash, the 2008 financial crisis, or the COVID-19 pandemic-induced market turmoil. Such underestimations can result in inadequate risk management strategies.

Given the widespread use of the Black-Scholes model and its extensions in the financial industry, particularly in the pricing of derivatives, understanding the limitations of its assumptions is crucial. According to [Bank for International Settlements (BIS), 2024], the notional value of the over-the-counter derivatives market has reached approximately $730 trillion. This highlights the potential global impact of mispricing and underestimating risks due to unrealistic assumptions.

To address these limitations, alternative models have been proposed that aim to capture more realistic dynamics of asset prices. One promising approach is to model price movements based on the interplay of supply and demand, which is driven by the collective behavior of market participants. This perspective naturally leads to the study of models inspired by statistical physics, where the interactions of many agents are explicitly considered. In the next section, we will introduce key concepts from statistical physics to formalize this approach.

2.2 Statistical physics: the Ising model

In this section, we introduce the Ising model as an example of model driven by the interaction of many agents (spins). The Ising model is a simple mathematical model of ferromagnetic materials. In its description, we will mostly follow the notation and tools presented in [Mézard and Montanari, 2009] and from professor Mézard's lecture notes. The model consists of Ising spins (that is, spins which can take binary values) on a d-dimensional cubic lattice (see figure 2.1). Mathematically, given a cubic lattice $\mathbb{L} = \{1, \dots, L\}^n$, we define an an Ising spin $\sigma_i \in \{-1, 1\}$ for each site $i \in \mathbb{L}$. Then, we can have any configuration $\underline{\sigma} = (\sigma_1, \dots, \sigma_n) \in \mathcal{X}_N = \{+1, -1\}^{\mathbb{L}}$.

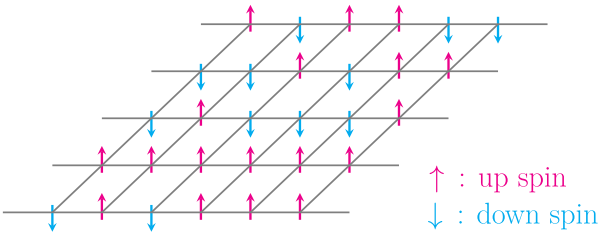

Figure 2.1: The Ising model on a 2D lattice.

The energy of a configuration $\underline{\sigma}$ is given by:

$$H(\underline{\sigma}) = -\sum_{\langle i,j \rangle} \sigma_i \sigma_j - B \sum_i \sigma_i \tag{2.8}$$

Where the sum over $\langle i, j \rangle$ is a sum over all nearest neighbors, and B is an external magnetic field. At equilibrium, the probability of a configuration $\underline{\sigma}$ is given by the Boltzmann distribution:

$$P(\underline{\sigma}) = \frac{e^{-\beta H(\underline{\sigma})}}{Z} \tag{2.9}$$

Where β is the inverse temperature, and Z is the partition function:

$$Z = \sum_{\underline{\sigma} \in \mathcal{X}_N} e^{-\beta H(\underline{\sigma})} \tag{2.10}$$

Interestingly, despite its simplicity, an analytical, closed-form solution for Z has been found only in the $d = 1$ and $d = 2$ cases. Higher dimensions remain unsolved, but numerical methods and mean-field approximations can be used to study the model in these cases.

One important quantity in the Ising model is the magnetization, which is defined as:

$$m = \frac{1}{N} \sum_i \langle \sigma_i \rangle \tag{2.11}$$

where $\langle \cdot \rangle$ denotes the average.

2.2.1 Solution of the Ising model in the one-dimensional case

For simplicity, assume $B = 0$. In the one-dimensional case, the Ising model can be solved exactly. Recall that:

$$H(\underline{\sigma}) = -\sum_{\langle i,j \rangle} \sigma_i \sigma_j \tag{2.12}$$

Then, the partition function is given by:

$$Z = \sum_{\underline{\sigma} \in \mathcal{X}_N} e^{-\beta H(\underline{\sigma})} = \sum_{\underline{\sigma} \in \mathcal{X}_N} e^{\beta \sum_{\langle i,j \rangle} \sigma_i \sigma_j} \tag{2.13}$$

Since each spin is connected to its nearest neighbors, we can write:

$$Z = \sum_{\underline{\sigma} \in \mathcal{X}_N} e^{\beta \sum_n \sigma_n \sigma_{n+1}} \tag{2.14}$$

Let us define $\tau_n = \sigma_{n-1}\sigma_n$. Then, $\sigma_n = \tau_n\tau_{n-1}\dots\tau_2\sigma_1$, which means that we can write:

$$\begin{aligned} Z &= \sum_{\sigma_1\in\{-1,1\}} \sum_{\tau_2,\dots\tau_n} e^{\beta\sum_n \tau_n} = 2\sum_{\tau_2,\dots,\tau_N} e^{\beta\sum_n\tau_n} \\ &= 2\sum_{\tau_2,\dots,\tau_N}\prod_n e^{\beta\tau_n} = 2(\sum_{\tau_2} e^{\beta\tau_2})\dots(\sum_{\tau_N} e^{\beta\tau_N}) \\ &= 2(2\cosh(\beta))^N \end{aligned} \tag{2.15}$$

Thus, we have found an analytical expression for the partition function in the one-dimensional case. The magnetization can be computed as:

$$m = \frac{1}{N}\sum_i \langle\sigma_i\rangle = \frac{1}{N}\frac{\partial}{\partial\beta}\log Z = \tanh(\beta) \tag{2.16}$$

2.2.2 The Curie-Weiss model

The Curie-Weiss model is a generalization of the Ising model, where instead of interacting with nearest neighbors, each spin interacts with all other spins. The Hamiltonian is given by:

$$H(\underline{\sigma}) = -\frac{J}{N}\sum_{i<j}\sigma_i\sigma_j - B\sum_i \sigma_i \tag{2.17}$$

The scaling factor $\frac{1}{N}$ is introduced to have a non-trivial free energy. This model is interesting because it introduced the concept of mean-field approximations. As usual, the partition function is given by:

$$\begin{aligned} Z &= \sum_{\underline{\sigma}\in\mathcal{X}_N} e^{-\beta H(\underline{\sigma})} \\ &= \sum_{\underline{\sigma}\in\mathcal{X}_N} e^{\beta\frac{J}{N}\sum_{i<j}\sigma_i\sigma_j + \beta B\sum_i\sigma_i} \\ &= \sum_{\underline{\sigma}\in\mathcal{X}_N} e^{\frac{1}{2}\beta\frac{J}{N}\sum_{i,j}\sigma_i\sigma_j + \beta B\sum_i\sigma_i - \frac{1}{2}\beta J} \\ &= \sum_{\underline{\sigma}\in\mathcal{X}_N} e^{\frac{1}{2}\beta\frac{J}{N}\left(\sum_i\sigma_i\right)^2 + \beta B\sum_i\sigma_i - \frac{1}{2}\beta J} \end{aligned} \tag{2.18}$$

Now, we can introduce the notation:

$$m(\underline{\sigma}) = \frac{1}{N}\sum_i \sigma_i \tag{2.19}$$

Then, we can rewrite the hamiltonian as:

$$H(\underline{\sigma}) = \frac{1}{2}JNm^2(\underline{\sigma}) + BNm(\underline{\sigma}) - \frac{1}{2}\beta J \tag{2.20}$$

And the partition function becomes:

$$\begin{aligned} Z &= \sum_{\underline{\sigma}\in\mathcal{X}_N} e^{\frac{1}{2}\beta JNm^2(\underline{\sigma})+\beta BNm(\underline{\sigma})-\frac{1}{2}\beta J} \\ &= \sum_{m} e^{\frac{1}{2}\beta JNm^2+\beta BNm-\frac{1}{2}\beta J}\mathcal{N}(m) \\ &= \sum_{m} e^{N\left(\frac{1}{2}\beta Jm^2+\beta Bm+\frac{1}{N}\log\mathcal{N}(m)\right)-\frac{1}{2}\beta J} \end{aligned} \tag{2.21}$$

Where $\mathcal{N}(m)$ is the number of configurations with magnetization m. Now, we can focus on the term $\frac{1}{N}\log\mathcal{N}(m)$, which in the large N limit we will call $S(m)$.

$$\begin{aligned} S(m) &= \lim_{N\to\infty}\frac{1}{N}\log\mathcal{N}(m) \\ &= \lim_{N\to\infty}\frac{1}{N}\log\frac{N!}{\left(\frac{1+m}{n}N\right)!\left(\frac{1-m}{n}N\right)!} \end{aligned} \tag{2.22}$$

Since, in order to get a magnetization m, we need exactly $\frac{1+m}{2}N$ spins up and $\frac{1-m}{2}N$ spins down, which can happen in $\binom{N}{\frac{1+m}{2}N}$ ways. Then, since we are interested in the large N limit, we can use Stirling's approximation:

$$\log n! \approx n\log n - n \tag{2.23}$$

Which allows us to rearrange and simplify the expression for $S(m)$:

$$S(m) = -\frac{1+m}{2}\log\left(\frac{1+m}{2}\right) - \frac{1-m}{2}\log\left(\frac{1-m}{2}\right) \tag{2.24}$$

Now, we recall the definition of the Shannon entropy:

Definition 5. *The Shannon entropy of a discrete probability distribution $p(x)$ is defined as:*

$$S(p) = -\sum_{x} p(x)\log p(x) \tag{2.25}$$

Where the sum is taken over all possible values of x. The Shannon entropy measures the amount of uncertainty or information in the distribution.

And we notice that $S(m)$ is the Shannon entropy of a Bernoulli distribution (binary random variable) with probability $p = \frac{1+m}{2}$ and $q = \frac{1-m}{2}$.

Now, in the large N limit, we notice the following:

- The increments of m become infinitesimal, allowing us to treat the sum as an integral.
- We can use the stirling approximation for the factorials, allowing us to subtitute $\frac{1}{N}\log\mathcal{N}(m)$ with $S(m)$.

- We can neglect the term $-\frac{1}{2}\beta J$ in the exponent, as it is $o(N)$.

Then, we can rewrite the partition function as:

$$Z \approx \int_{-1}^{1} dm e^{N\phi(m)}, \quad \text{where } \phi(m) = \frac{1}{2}\beta J m^2 + \beta B m + S(m) \tag{2.26}$$

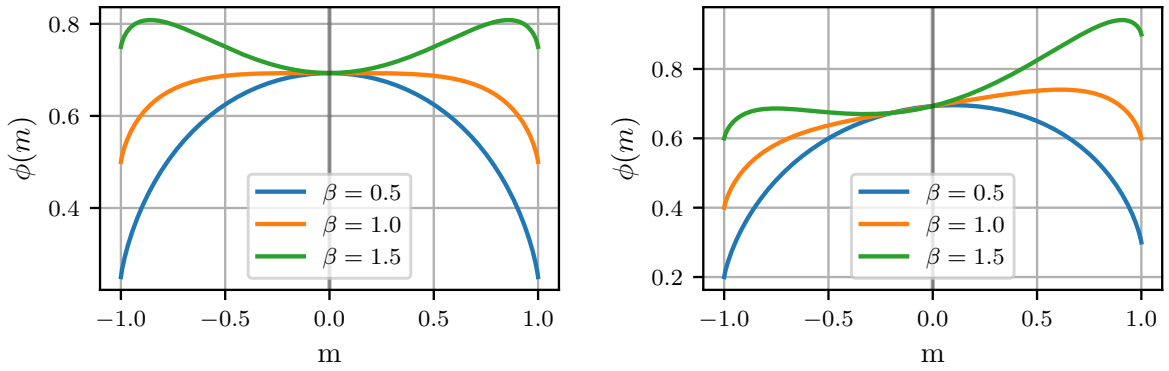

Figure 2.2: The function $\phi(m)$ defined in Equation 2.26 for $B = 0$ (left) and $B = 0.1$ (right).

Using the laplace approximation, we see that the integral is dominated by the maximum of $\phi(m)$, which we will call m_0.

$$\begin{aligned} &\frac{d}{dm}\phi(m_0) = 0 \\ \implies &\beta J m_0 + \beta B + \frac{1}{2}\left(\log\frac{1-m}{1+m}\right) = 0 \\ \implies &\operatorname{arctanh}(m_0) = \beta J m_0 + \beta B \end{aligned} \tag{2.27}$$

Thus, we have found the mean-field equation for the Curie-Weiss model:

$$m = \tanh(\beta J m + \beta B) \tag{2.28}$$

This equation is similar to the one we found for the Ising model in Equation 2.16, however, this time we have a phase transition. In Figure 2.3 we can see that, for different value of β, we can have one or three solutions to the equation. In the case of $B = 0$, we can have one solution for $\beta < \beta_c$ and three solutions for $\beta > \beta_c$. The critical value of β is given by:

$$\beta_c = \frac{1}{J} \tag{2.29}$$

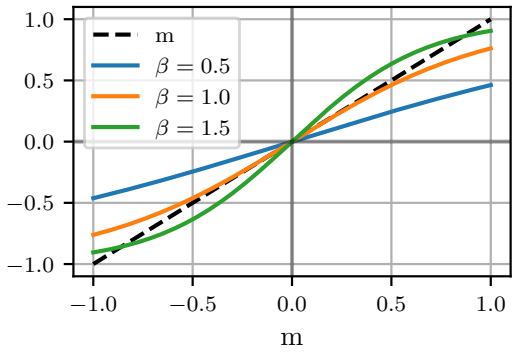

Figure 2.3: The left-hand side and right-hand side of Equation 2.28 for $B = 0$ plotted for different values of β. Intersecting points correspond to solutions of the equation.

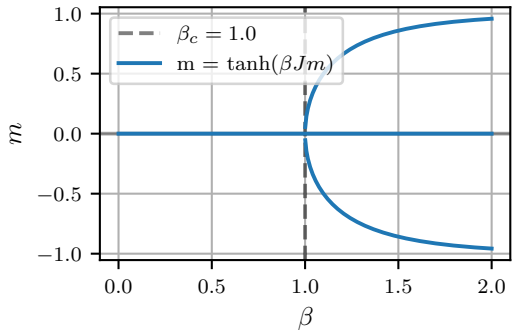

Figure 2.4: Solutions to Equation 2.28 with respect to the inverse temperature β for $B = 0$.

Chapter 3

The Bornholdt model

In the spirit of finding a model for the price dynamics of risky assets, we now present the model proposed in [Bornholdt, 2001]. The idea is to formulate a model with maximum simplicity, which includes the possibility of strategic interaction between agents in the market.

3.1 Introduction

3.1.1 Financial motivation

In [Bornholdt, 2001], a simple spin model, which we will refer to as the Bornholdt model, is proposed to model trading in financial markets. In the model, agents are seen as interacting spins, which have two possible actions: buy or sell an asset. The choice of each agent is influenced by two contrasting forces:

- "Do what your neighbors do": this is the strategy that momentum traders follow. They try to follow the trend in the market, buying when the price is rising and selling when it is falling.
- "Do what the minority does": this is the strategy that mean-reversion traders follow. They try to buy when the price is falling and sell when it is rising, betting on a reversal of the trend.

We will see how these two strategies are implemented in the model.

3.1.2 Model definition

Consider a model with N spins with orientations $\sigma_i \in \{-1, +1\}$, representing the decision of agent i to buy or sell a stock. We will consider updates following a heat-bath dynamics:

$$\begin{aligned} \sigma_i(t+1) &= +1 \text{ with } \; p = \frac{1}{1+e^{-2\beta h_i(t)}} \\ \sigma_i(t+1) &= -1 \text{ with } \; 1-p \end{aligned} \tag{3.1}$$

Where $h_i(t)$ is the local field of agent i at time t:

$$h_i(t) = \sum_{j=1}^{N} J_{ij}\sigma_j - \alpha C_i(t)\frac{1}{N}\sum_{j=1}^{N}\sigma_j(t) \tag{3.2}$$

Where J_{ij} is the coupling between agents i and j, σ_j is the agent's action at t, $C_i(t)$ is the strategy of i at time t, and α is a parameter. The first term in the local field pushes the agent to follow the trend of spins in their proximity (do what your neighbors do), while the second term pushes the agent to follow the minority (do what the minority does), assuming the strategy $C_i(t)$ is positive. If we consider the case in which $C_i(t) = 1 \; \forall i, t$, we have that each trader follows both a momentum and a mean-reversion strategy simultaneously. This leads to near-vanishing magnetization even for temperatures below the critical temperature. We will focus on the more interesting and realistic case in which the strategies are updated at each time by each agent. Specifically, we will assume that a trader in the majority will try to switch to the minority strategy and thus adopt $C_i(t+1) = +1$, while a trader in the minority will try to switch to the majority strategy and thus adopt $C_i(t+1) = -1$. This is a reasonable assumption, as traders in the minority are likely to be more cautious and risk-averse, while traders in the majority are likely to be more aggressive and willing to take risks. This dynamics is then described by:

$$C_i(t+1) = \begin{cases} +1 & \text{if} \quad \alpha\sigma_i(t)\sum_{j=1}^{N}\sigma_j(t) > 0 \\ -1 & \text{otherwise} \end{cases} \tag{3.3}$$

Rearranging the equation, we can write:

$$C_i(t+1) = \begin{cases} +C_i(t) & \text{if} \quad \alpha\sigma_i(t)C_i(t)\sum_{j=1}^{N}\sigma_j(t) > 0 \\ -C_i(t) & \text{otherwise} \end{cases} \tag{3.4}$$

Now, we can take one extra step and assume that the strategy update is done instantaneously, so that we can write:

$$C_i(t) = \begin{cases} +C_i(t) & \text{if} \quad \alpha\sigma_i(t)C_i(t)\sum_{j=1}^{N}\sigma_j(t) > 0 \\ -C_i(t) & \text{otherwise} \end{cases} \tag{3.5}$$

Then, substituting this into the local field, we have a remarkably simple expression for the local field:

$$h_i = \sum_{j=1}^{N} J_{ij}\sigma_j - \alpha\sigma_i \left| \frac{1}{N}\sum_{j=1}^{N}\sigma_j \right| \tag{3.6}$$

Then, the hamiltonian of the model is:

$$\begin{aligned} H(\underline{\sigma}) &= -\sum_{i=1}^{N}\sigma_i h_i \\ &= -\sum_{i,j} J_{i,j}\sigma_i\sigma_j + \frac{\alpha}{N}\sum_{i=1}^{N}\sigma_i \left|\sum_{j=1}^{N}\sigma_j\right| \end{aligned} \tag{3.7}$$

At this point, the magnetization $M = \frac{1}{N}\sum_{j=1}^{N}\sigma_j$ can be interpreted as the price of the security that is being traded. We seek to study the dynamics of the model.

3.1.3 Analysis of the model

We will focus on the fully connected case in which $J_{i,j} = \frac{J}{N}\ \forall i, j$. The hamiltonian of the model is then:

$$H(\underline{\sigma}) = -\frac{J}{N}\sum_{i,j}\sigma_i\sigma_j + \frac{\alpha}{N}\sum_{i=1}^{N}\sigma_i \left|\sum_{j=1}^{N}\sigma_j\right| \tag{3.8}$$

We will proceed in a similar way as in Section 2.2.2, by introducing a combinatorial factor $\mathcal{N}(m)$ and taking the large N limit.

The partition function of the model is given by:

$$\begin{aligned} Z &= \sum_{\underline{\sigma}\in\mathcal{X}_N} e^{-\beta H(\underline{\sigma})} \\ &= \sum_{\underline{\sigma}\in\mathcal{X}_N} e^{-\beta\frac{J}{N}\sum_{i,j}\sigma_i\sigma_j + \beta\frac{\alpha}{N}\sum_{i=1}^{N}\sigma_i\left|\sum_{j=1}^{N}\sigma_j\right|} \\ &= \sum_{\underline{\sigma}\in\mathcal{X}_N} e^{-\beta\frac{J}{N}\left(\sum_i\sigma_i\right)^2 + \beta\frac{\alpha}{N}\sum_{i=1}^{N}\sigma_i\left|\sum_{j=1}^{N}\sigma_j\right|} \end{aligned} \tag{3.9}$$

Now, we can introduce the notation:

$$m(\underline{\sigma}) = \frac{1}{N}\sum_i \sigma_i \tag{3.10}$$

Then, we can rewrite the hamiltonian as:

$$H(\underline{\sigma}) = -JNm^2(\underline{\sigma}) + \alpha N m(\underline{\sigma})\,|m(\underline{\sigma})| \tag{3.11}$$

And the partition function becomes:

$$\begin{aligned} Z &= \sum_{\underline{\sigma}\in\mathcal{X}_N} e^{N\left(\beta J m^2(\underline{\sigma}) + \beta\alpha m(\underline{\sigma})|m(\underline{\sigma})|\right)} \\ &= \sum_{m} e^{N\left(\beta J m^2 + \beta\alpha m|m|\right)}\mathcal{N}(m) \\ &= \sum_{m} e^{N\left(\beta J m^2 + \beta\alpha m|m| + \frac{1}{N}\log\mathcal{N}(m)\right)} \end{aligned} \tag{3.12}$$

Where $\mathcal{N}(m)$ is the number of configurations with magnetization m. In Section 2.2.2, we have seen that $S(m) := \lim_{N\to\infty}\frac{1}{N}\log\mathcal{N}(m)$ is the Shannon entropy of a bernoulli distribution with probability $p = \frac{1+m}{2}$ and $q = \frac{1-m}{2}$.

Then, in the large N limit, we notice the following:

- The increments of m become infinitesimal, allowing us to treat the sum as an integral.
- We can subtitute $\frac{1}{N}\log\mathcal{N}(m)$ with $S(m)$.

Then, we can rewrite the partition function as:

$$Z \approx \int_{-1}^{1} dm e^{N\phi(m)}, \quad \text{where } \phi(m) = \beta J m^2 + \alpha m|m| + S(m) \tag{3.13}$$

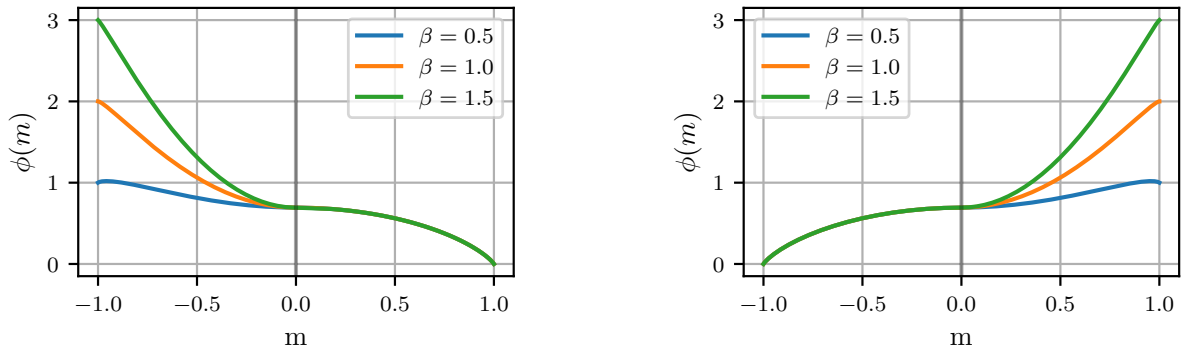

Figure 3.1: The function $\phi(m)$ defined in Equation 3.13 for different values of β, with $J = 1$ and $\alpha = 1$ (left) and $\alpha = -1$ (right).

We now aim to rewrite $\phi(m)$ in a more convenient form. First, we notice that:

$$x|x| = x^2(2\theta(x) - 1) \tag{3.14}$$

Where $\theta(x)$ is the Heaviside step function:

$$\theta(x) = \begin{cases} 0 & \text{if } x < 0 \\ 1 & \text{if } x \geq 0 \end{cases} \tag{3.15}$$

Which we can write as:

$$\theta(x) = \int_{-\infty}^{x} \delta(t)dt \tag{3.16}$$

Then, we can rewrite $\phi(m)$ as:

$$\phi(m) = \beta J m^2 + \alpha m^2(2\theta(m) - 1) + S(m) \tag{3.17}$$

Without going into the technical details, writing $\phi(m)$ in this way allows us to take its weak derivative and obtain the saddle point equation:

$$\begin{aligned} &\frac{d\phi(m)}{dm} = 0 \\ \implies &2\beta J m - 2\alpha\beta m^2\delta(m) - 4\alpha\beta m\theta(m) + 2\alpha\beta m + \frac{1}{2}\log\frac{1-m}{1+m} = 0 \\ \implies &2\beta J m - 4\alpha\beta m\theta(m) + 2\alpha\beta m = \operatorname{arctanh}(m) \end{aligned} \tag{3.18}$$

From which we get the self-consistent equation:

$$m = \tanh\left(2\beta J m - 4\alpha\beta m\theta(m) + 2\alpha\beta m\right) \tag{3.19}$$

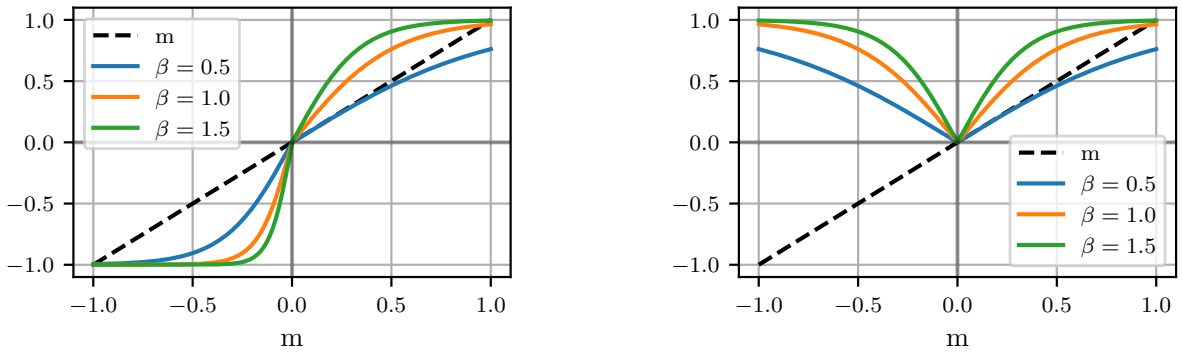

Figure 3.2: The left-hand side and right-hand side of Equation 3.19 for $J = 1$ and $\alpha = 1$ (left) and $\alpha = -1$ (right). Intersecting points correspond to solutions of the equation.

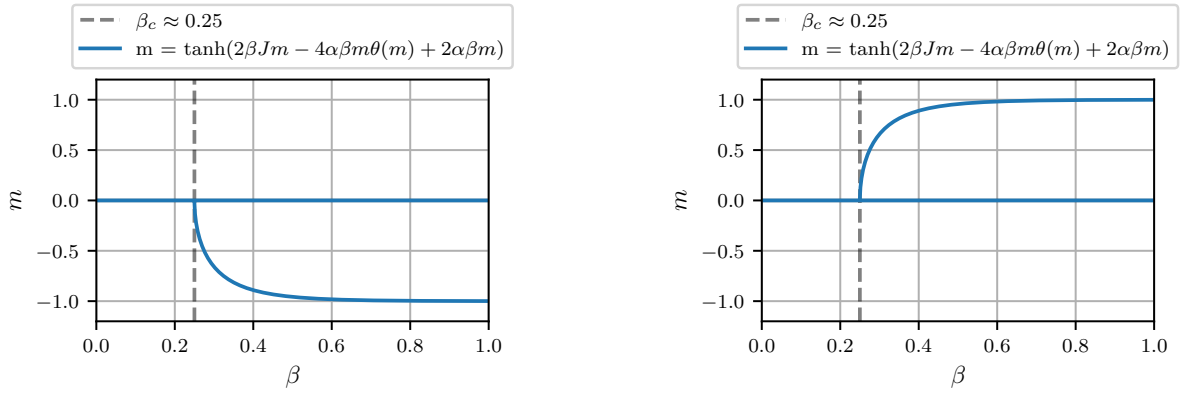

Figure 3.3: Solutions of Equation 3.19 for different values of β, with $J = 1$ and $\alpha = 1$ (left) and $\alpha = -1$ (right). The critical temperature is indicated by the dashed line.

3.2 Simulations of the Bornholdt model

We conducted a numerical simulation of the Bornholdt model, employing a system consisting of 1024 spins arranged in a two-dimensional square lattice. The coupling constant was set to $J = 1.0$, the external field parameter was $\alpha = 4.0$, and the temperature of the system was defined as $T = 1/\beta = 1.5$. The simulation was carried out over a sufficiently large number of time steps to allow the results to be representative of the model's long-term dynamics.

3.2.1 Only fundamental traders

We start by analysing the case in which all agents are fundamental traders, meaning that they all follow the same strategy. In this case, we set $C_i(t) = 1$ for all agents and all times. The results of the simulation are shown in figure 3.4. As expected, the system is stuck in a noisy state in which the magnetization fluctuates between low positive and negative values.

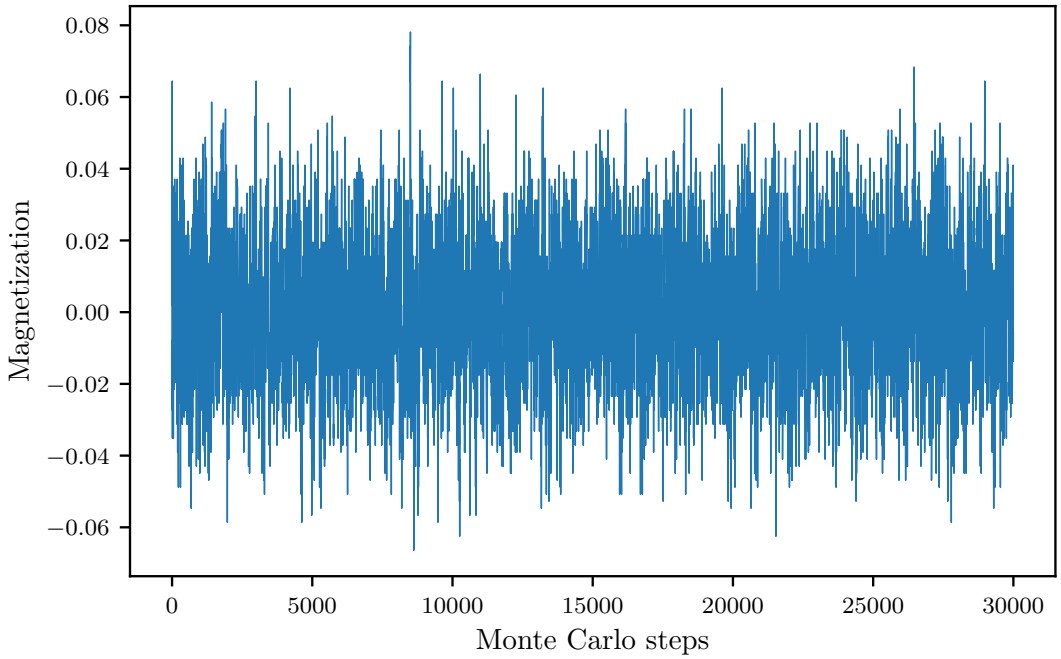

Figure 3.4: Dynamics of the magnetization of the system with only fundamental traders.

3.2.2 Dynamics of the strategies

The simulations indicate that the initial distribution of agents' strategies has a negligible long-term impact on the system's behavior. Regardless of the starting configuration, the system quickly converges to a stable state where approximately 50% to 70% of agents adopt the strategy $C_i(t) = 1$. This convergence is evident from the dynamics shown in figure 3.5. Consequently, for the purposes of simulating the model, it is not necessary to distinguish between different initial distributions of strategies, as the system's evolution is largely independent of these initial conditions.

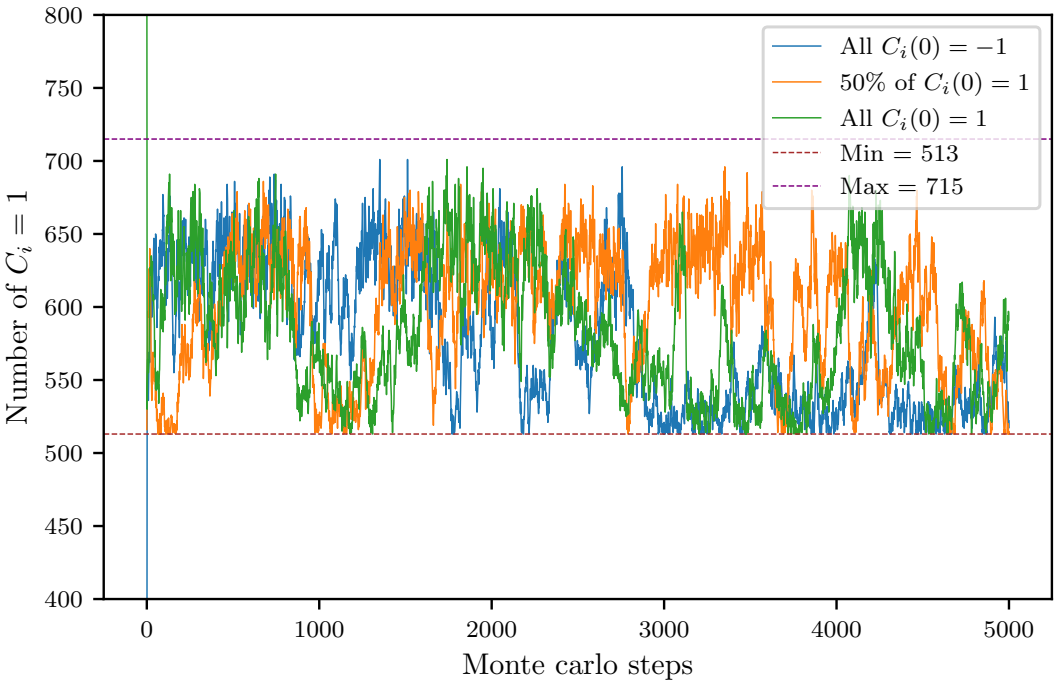

Figure 3.5: Dynamics of agent's strategy based on different starting distributions.

3.2.3 Dynamics of the price

Following the interpretation proposed in [Bornholdt, 2001], the magnetization of the system is treated as the price of a financial asset being traded by the agents. By plotting the magnetization as a function of time, we obtain a time-series that mimics the price dynamics of a financial asset. This is illustrated in figure 3.6, where the temporal evolution of the magnetization is shown.

In addition to examining the magnetization (i.e., the price), it is also insightful to analyze the underlying configuration of spins that produces this magnetization. The spin configuration provides a microscopic view of the system's state, which complements the macroscopic perspective offered by the magnetization. As shown in figure 3.7, the system alternates between two distinct regimes: metastable states, where the spin configuration remains relatively stable over time, and turbulent states, characterized by rapid and chaotic changes in the spin configuration. These alternating regimes highlight the complex dynamics of the system and their influence on the observed price behavior.

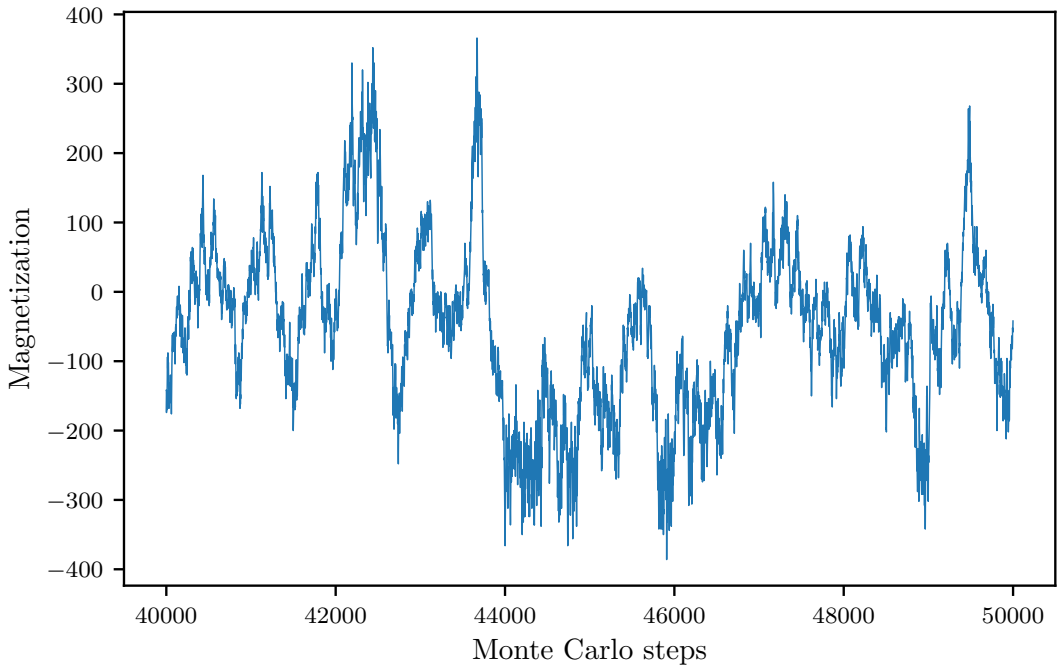

Figure 3.6: Dynamics of the magnetization of the system.

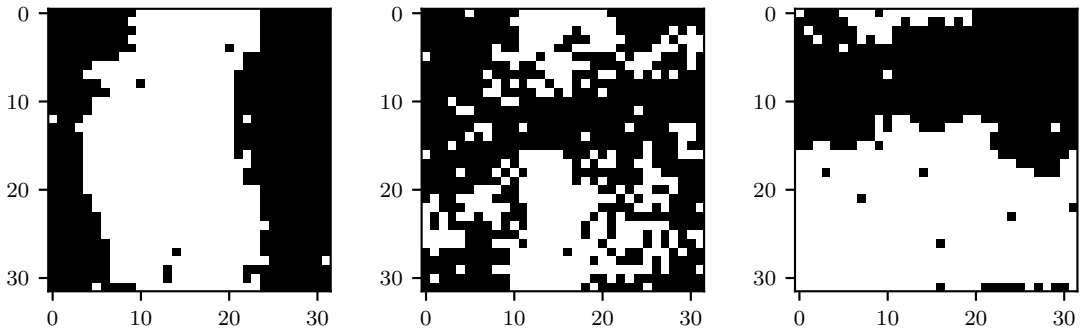

Figure 3.7: Snapshots of the lattices at times $t = 43400$, $t = 43700$ and $t = 43850$.

3.2.4 Dynamics and statistical properties of the returns

To analyze the dynamics of the returns of the asset, we define the log-returns as the logarithm of the ratio of the magnetization at consecutive time steps. Since the magnetization $M(t)$ can take on both positive and negative values, we use its absolute value to ensure that the log-returns are well-defined. Additionally, to avoid issues with division by zero or taking the logarithm of zero, we introduce a small positive constant ϵ, where $\epsilon \ll 1$. The log-returns are then computed as:

$$R(t) = \log\left(\frac{|M(t)| + \epsilon}{|M(t-1)| + \epsilon}\right) \tag{3.20}$$

Here, $R(t)$ represents the return at time t, $M(t)$ is the magnetization at time t, and ϵ is a small constant added for numerical stability.

The resulting time-series of the returns is shown in figure 3.8.

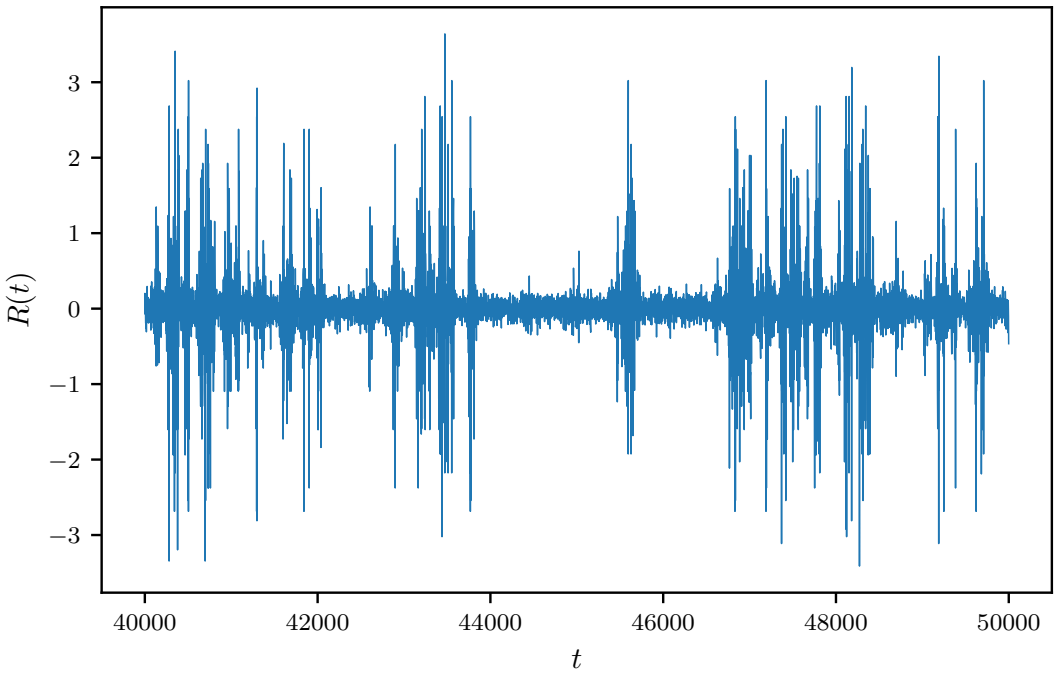

Figure 3.8: Time-series of the returns of the asset.

From a financial perspective, we are interested in checking whether the returns exhibit the statistical properties of real financial data, namely fat tails and autocorrelation, as noted in [Bouchaud and Potters, 2000].

Fat tails

The analysis of the distribution of the returns, as illustrated in figures 3.9 and 3.10, provides strong evidence that the returns exhibit fat tails. This characteristic is a hallmark of financial time-series and indicates that extreme events (large positive or negative returns) occur more frequently than would be expected under a normal distribution.

To further investigate this property, we compare the returns to a normal distribution using a QQ-plot, shown in figure 3.11. The QQ-plot clearly demonstrates significant deviations from the straight line that would be expected if the returns were normally distributed. These deviations, particularly in the tails, confirm the presence of fat tails in the distribution.

Additionally, we perform a statistical test to formally assess whether the returns follow a normal distribution. Specifically, we use the Shapiro-Wilk test, which tests the null hypothesis that the data is drawn from a normal distribution. The results of the test yield a p-value on the order of 10^{-192}. Such an extremely small p-value indicates that we can

reject the null hypothesis with extremely high confidence, confirming that the returns are not normally distributed. Additionally, we compute the kurtosis of the returns, which is approximately 24.2. This value indicates an extremely leptokurtic distribution, suggesting a very high likelihood of outliers. [Chiang and Li, 2007] shows that stocks in the Dow Jones Industrial Average show kurtosis values ranging from 1.08 to 24.13. This means we could see the price movements of the Bornholdt model as a very volatile stock.

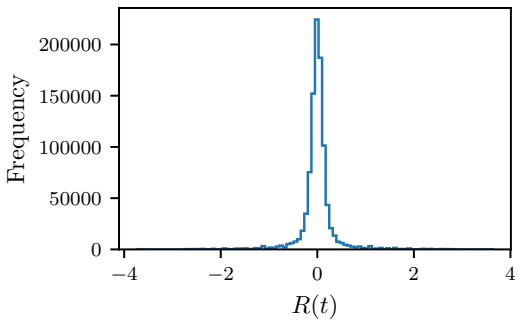

Figure 3.9: Distribution of the returns of the asset.

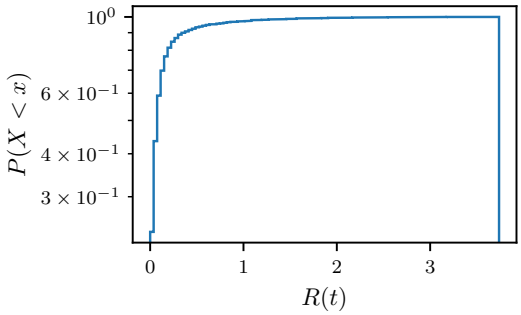

Figure 3.10: Cumulative distribution of the returns of the asset.

Autocorrelation

From figure 3.8, we can already seen that the periods of high volatility (i.e. large positive or negative returns) tend to be clustered together. This is a sign of autocorrelation in the returns. To quantify this, we can compute the autocorrelation function of the returns, defined as

$$\rho(k) = \frac{\sum_{t=1}^{N-k}(R(t) - \bar{R})(R(t+k) - \bar{R})}{\sum_{t=1}^{N}(R(t) - \bar{R})^2} \tag{3.21}$$

where N is the number of returns, $R(t)$ is the return at time t, and $\bar{R}$ is the mean of the returns. The autocorrelation function measures the correlation between the returns at time t and time $t + k$. A positive value of $\rho(k)$ indicates that the returns at time t and time $t + k$ are positively correlated, while a negative value indicates that they are negatively correlated. A value close to zero indicates that there is no correlation between the returns at time t and time $t + k$. The autocorrelation function is computed for lags $k = 1, 2, \ldots, 100$ and is shown in figure 3.12. The results show that the autocorrelation is significant for a large number of lags, which is consistent with the empirical observation that financial returns are autocorrelated.

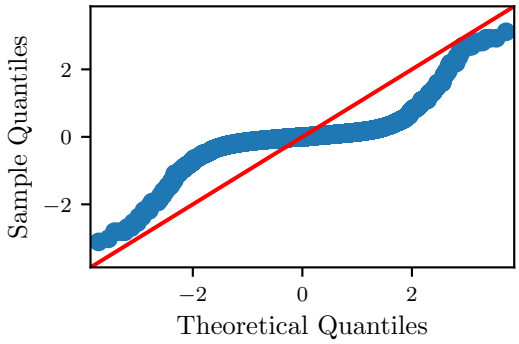

Figure 3.11: QQ-plot of the returns against a normal distribution.

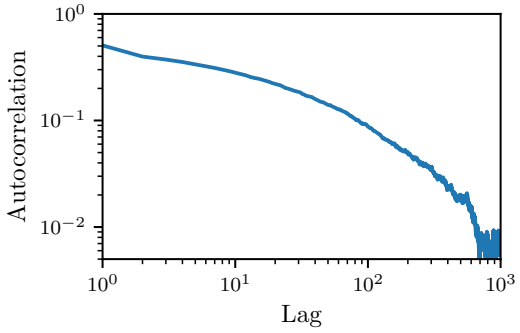

Figure 3.12: Autocorrelation function of the returns.

3.3 Discussion

The results of the simulation suggest that the Bornholdt model is able to reproduce some of the statistical properties of real financial data, such as fat tails and autocorrelation of returns. This is interesting because the model is based on a simple spin model, and does not rely on any assumptions about the rationality of agents or the efficiency of markets.

As seen in 2.1, one of the main assumptions of the model introduced in [Black and Scholes, 1973] is that the price of the underlying asset follows a geometric Brownian motion. The Bornholdt model, however, results in price dynamics which exhibit fat tails, and do not have independent increments, as shown by the autocorrelation of the returns, which is the case also in real financial data.

The key observation here is that, unlike in a geometric Brownian motion, the price (i.e. magnetization) at time t is not enough to describe the distribution of prices at times $t+s,\ s \geq 0$. This might be counterintuitive, as by equation 3.1, the future configuration of spins is determined by the current configuration of spins. However, it is important to note that the current magnetization is not enough to determine the current configuration of spins. In fact, the magnetization is a global property of the system, while the configuration can vary locally. In figures 3.13 and 3.14, we can see that the magnetization is the same at times $t = 129722$ and $t = 130293$, but the configuration of spins is completely different.

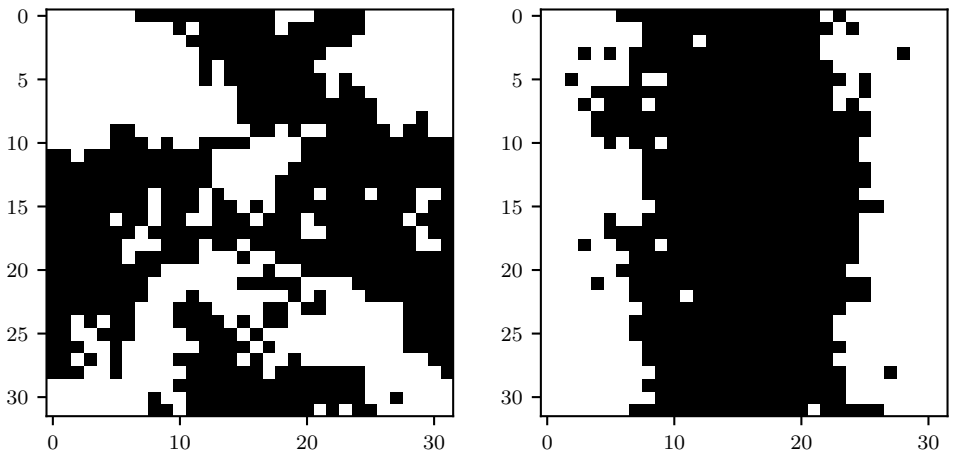

Figure 3.13: Snapshots of the lattices at times $t = 129722$, and $t = 130293$.

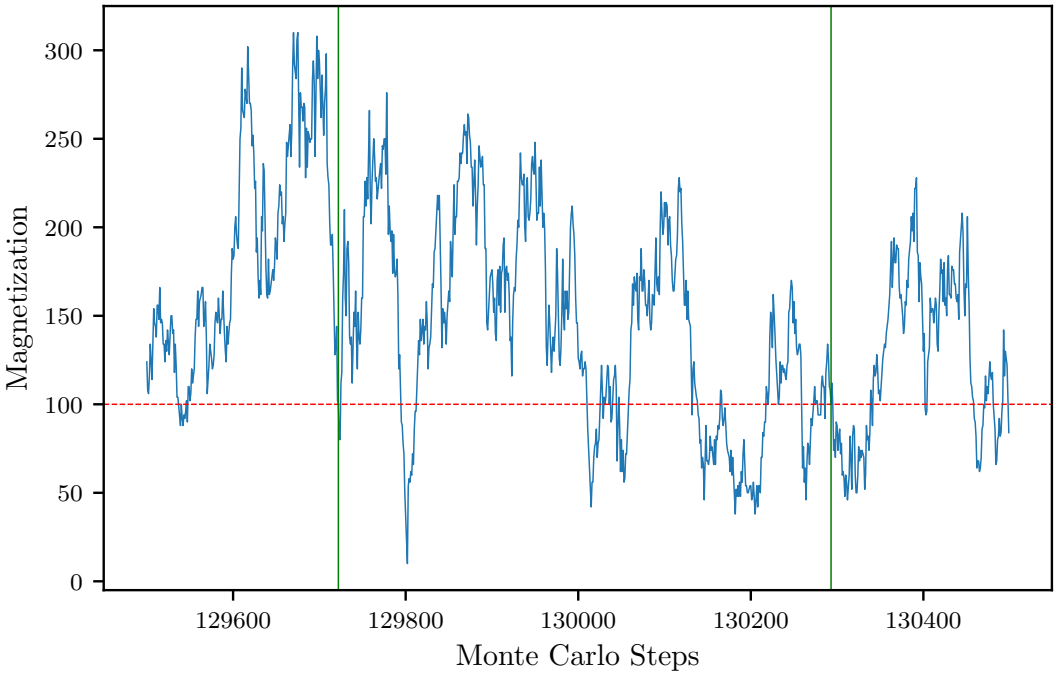

Figure 3.14: Dynamics of the magnetization of the system. The green lines represent the times at which the snapshots in figure 3.13 were taken.

Chapter 4

Conclusion

In this work, we have briefly introduced the formal languages of financial mathematics and statistical physics, in order to challenge the common assumption that prices of risky assets follow a geometric Brownian motion with constant volatility.

Looking for a more realistic model, we have introduced the Bornholdt model, which takes into account the interaction between agents when modelling price dynamics. We have shown that, empirically, the model is able to reproduce the stylized facts of financial time series, such as the power law distribution of returns and the volatility clustering phenomenon.

However, this model does not come without its limitations, both in terms of the assumptions made and the analytical tractability. In what is perhaps the biggest limitation, we have chosen the magnetization as a proxy for the price, with the clear limitation that while prices can take values in $\mathbb{R}^+$, the magnetization is bounded between -1 and 1. Additionally, the agents in the model are restricted between the binary states of either buying or selling, without allowing for the possibility of holding a position, as well as neglecting the different volumes of trades which investors might make.

Another limitation of the model is that, unlike geometric Brownian motion, the Bornholdt model does not have the same level of analytical tractability. Oftentimes, traders are fully aware of the unrealistic assumptions of their models, but still choose them for their straight-forward derivation.

Ideally, future work could focus on extending the Bornholdt model to include more realistic features of financial markets, such as the possibility of holding a position, the volume of trades, and the inclusion of transaction costs to name a few. Additionally, it would be interesting to explore which assumptions could be relaxed in order to obtain a more tractable model, while still being able to reproduce the stylized facts of financial time series.

Bibliography

[Bachelier, 1900] Bachelier, L. (1900). Théorie de la spéculation. *Annales scientifiques de l'École Normale Supérieure*, 3(17):21–86.

[Bank for International Settlements (BIS), 2024] Bank for International Settlements (BIS) (2024). OTC derivatives statistics. Accessed April 10, 2025.

[Black and Scholes, 1973] Black, F. and Scholes, M. (1973). The pricing of options and corporate liabilities. *Journal of Political Economy*, 81(3):637–654.

[Bornholdt, 2001] Bornholdt, S. (2001). Expectation bubbles in a spin model of markets: Intermittency from frustration across scales. *International Journal of Modern Physics C*, 12(05):667–674.

[Bouchaud and Potters, 2000] Bouchaud, J. and Potters, M. (2000). *Theory of Financial Risks: From Statistical Physics to Risk Management*. Theory of Financial Risks: From Statistical Physics to Risk Management. Cambridge University Press.

[Bouchaud and Mézard, 2000] Bouchaud, J.-P. and Mézard, M. (2000). Wealth condensation in a simple model of economy. *Physica A: Statistical Mechanics and its Applications*, 282(3):536–545.

[Chiang and Li, 2007] Chiang, T. and Li, J. (2007). Empirical analysis of asset returns with skewness, kurtosis, and outliers: Evidence from 30 dow-jones industrial stocks.

[Mantegna and Stanley, 1999] Mantegna, R. N. and Stanley, H. E. (1999). *Introduction to Econophysics: Correlations and Complexity in Finance*. Cambridge University Press.

[Mézard and Montanari, 2009] Mézard, M. and Montanari, A. (2009). *Information, Physics, and Computation*. Oxford University Press.

[Sharma et al., 2011] Sharma, B. G., Agrawal, S., Sharma, M., Bisen, D. P., and Sharma, R. (2011). Econophysics: A brief review of historical development, present status and future trends.

Unless otherwise stated, all figures are created by the author. Figure 2.1 is adapted from the original by Ta2o, CC BY 4.0, via Wikimedia Commons `https://upload.wikimedia.org/wikipedia/commons/f/fe/2D_ising_model_on_lattice.svg`